J Intell Robot Syst
DOI 10.1007/s10846-012-9717-2

Design and Validation of an $\mathcal{L}_1$ Adaptive Controller for Mini-UAV Autopilot

Elisa Capello · Giorgio Guglieri · Fulvia Quagliotti · Daniele Sartori

Received: 7 May 2012 / Accepted: 12 July 2012

Abstract The dynamics of Unmanned Aerial Vehicles (UAVs) is nonlinear and subject to external disturbances. The scope of this paper is the test of an $\mathcal{L}_1$ adaptive controller as autopilot inner loop controller candidate. The selected controller is based on piecewise constant adaptive laws and is applied to a mini-UAV. Navigation outer loop parameters are regulated via PID control. The main contribution of this paper is to demonstrate that the proposed control design can stabilize the nonlinear system, even if the controller parameters are selected starting from a decoupled linear model. The main advantages of this technique are: (1) the controller can be implemented for both linear and nonlinear systems without parameter adjustment or tuning procedure, (2) the controller is robust to unmodeled dynamics and parametric model uncertainties. The design scheme of a customized autopilot is illustrated and different configurations (in terms of mass, inertia and airspeed variations) are analyzed to validate the presented approach.

Keywords UAVs · Adaptive controller · Autopilot design

E. Capello (✉) · G. Guglieri · F. Quagliotti · D. Sartori
Dipartimento di Ingegneria Meccanica e Aerospaziale, Politecnico di Torino,
Corso Duca degli Abruzzi 24,
10129 Torino, Italy
e-mail: elisa.capello@polito.it

G. Guglieri
e-mail: giorgio.guglieri@polito.it

F. Quagliotti
e-mail: fulvia.quagliotti@polito.it

D. Sartori
e-mail: daniele.sartori@polito.it

1 Introduction

Unmanned Aerial Vehicles (UAVs) represent an ideal platform for testing advanced control techniques. In recent years, many researches regarding the design of UAV autopilot algorithms using modern control theories have been completed. Most of the modern autopilots incorporate controller algorithms to meet the always more demanding requirements of flight maneuvers and mission accomplishment. However, due to the complexity and the computational need of the control algorithms, most of the commercial autopilots are based on Proportional Derivative Integrative (PID) philosophy. The scope of the present research paper is the implementation of an adaptive controller that is robust in presence of model uncertainties due to platform geometric and inertial variations which occur during the flight tests (such as variations on payload mass). The simple structure, the reduced presence of

Published online: 04 August 2012

oscillations during the implementation and a minimum computation effort make the $\mathcal{L}_1$ adaptive controller the ideal candidate for an autopilot control law. Two cases are analyzed: (1) a linear decoupled state space model for a specific flight condition and (2) a nonlinear model obtained from the complete equations of motion. In both cases a two loop controller is implemented. The inner loop is synthesized using an $\mathcal{L}_1$ adaptive algorithm for pitch, roll and airspeed control; the outer loop instead is based on PIDs to control altitude and heading.

As explained in [1], different and advanced control techniques have been implemented in autopilot systems to guarantee the desired performance. Most commercial autopilots are based on PID controllers because they are easy to tune and to understand. Moreover, by using PIDs the designers have a good control of the system dynamics. In detail, starting with proportional gain and adding integral and derivative terms, the designers can obtain a zero steady state error for a step input and a fast time response. Many methods for PID tuning can be found in literature, [2] and [3] provide a good review of different robust and optimal techniques. In the last years, some researchers have focused the attention on the development of automatic tuning and adaptation techniques for the definition of the PID gains. For example, [4] have proposed a computationally efficient procedure for H_∞ PID optimal design instead of brute force search. The method proposed in Ho's paper revealed important structural properties of H_∞ PID controllers. Authors of [5] have proposed a set of simple closed formulas for the explicit computation of the parameters in finite terms. They eliminate graphical, heuristic and trial and error procedures to verify the robustness of the selected parameters. The main drawback of PID autopilot is its lack of adaptivity due to the changes in the UAV dynamics. This means that the PID parameters need to be retuned in the presence of wind disturbances or in case the payload characteristics are changed. For this reason adaptive controllers could be a good candidate for the control of autonomous UAV flight.

A variety of adaptive control techniques have been proposed for the derivation of autopilot inner loops. Researchers in [6] implemented a two-loop controller where the inner loop is a dynamic inversion controller with an adaptive neural network and the outer loop is a LQR controller. Similarly, [7] presented the implementation of an adaptive neural network controller for autonomous flight. However, traditional model-based adaptive controllers may not be applicable since they are generally useful on the condition that the system dynamics are linear-in-the-parameters. In [8] the authors presented an alternative adaptive controller based on neural networks using backstepping technique. The main feature of [8] is that the adaptive controller is designed assuming that all of the nonlinear functions of the system have uncertainties and the neural network weights are adjusted adaptively via Lyapunov theory. Similarly, [9] derived an adaptive backstepping approach for the longitudinal aircraft control and a Lyapunov analysis of the stability properties of the closed loop system was considered. Paper [10] extended the case presented by [9] including the control of the roll channel. As explained in the previous references, even if Lyapunov techniques assure the convergence of the tracking error and low computational effort is required, they do not necessarily ensure parameter convergence. The authors of [11] proposed an $\mathcal{L}_1$ adaptive pitch controller for a mini UAV and validated the proposed algorithm in experimental flight tests. The $\mathcal{L}_1$ adaptive control methodology addresses some of the problems exhibited by traditional adaptive control approaches by providing fast and robust adaptation, simultaneously leading to desired transient performance for the system input and output signals, in addition to steady-state tracking. The decoupling between fast adaptation and robustness is achieved via the introduction of a low-pass filter on the adaptive control signal. This key element can be based on robustness and performance specifications. The complete theory is presented in [12, 13]. A drawback of [11] is the implementation and validation of a single loop (a pitch attitude hold).

Compared with the existing results previously discussed, a contribution of the present paper is the validation of the controller parameters when a nonlinear complete aircraft model is considered (both longitudinal and latero-directional planes), including model uncertainties and unmodeled

dynamics. The control laws are derived and tuned starting from a linear and decoupled state space model, designed for a specific flight condition. An initial comparison with a robustly optimized PID controller show that the $\mathcal{L}_1$ controller achieves better performance in controlling the linear aircraft model. The authors also demonstrate that, using a lower fidelity model (linear) which is significantly different from the high fidelity model (nonlinear), the $\mathcal{L}_1$ controller is robust to the model changes and a gain retuning is not required. Moreover, the effectiveness of the controller parameters is demonstrated for different flight and inertial configurations. Uncertainties related to flight conditions (variations on speed V and mass m) take into account the presence of turbulence during the real flight, the need to cover a large portion of flight envelope and variations on payload mass which occur during the flight tests. Variations on inertial data J take into account platform modeling inaccuracies arising during the manufacturing process. Another important advantage is that the PID gains both for the altitude and heading hold loop are tuned on the linear case, thus an additional gain tuning for the outer loop is not required.

The paper is organized as follows. The models used for the controller design and for the simulations are described in Section 2. In Section 3 the $\mathcal{L}_1$ adaptive controller theory is presented. Some experimental results are analyzed in Section 4. In this section both linear and nonlinear cases are considered, validation with parameters variation is included. Conclusions are presented in Section 5.

2 Aircraft and Autopilot Description

The aircraft considered for the controller implementation is the MH850 mini-UAV [14, 15]. The MH850 is characterized by tailless configuration, electric propulsion, tractor propeller and non-movable vertical fins at wingtips (see Fig. 1). The wingspan is 85 cm, the approximate mass 1 kg, it is able to fly for 45 min at a cruise speed of 13.5 m/s. Aircraft control is achieved with trailing edge elevon (symmetric deflection for elevator δ_e and antisymmetric for aileron δ_a). This aircraft has enough specific excess power to climb with non-marginal rates at altitude. A numerically derived database comprehensive of all aerodynamic derivatives is employed to build the linear and nonlinear aircraft models.

Fig. 1 The MH850 mini-UAV

The MH850 aircraft is able to perform autonomous flight thanks to the on board installation of an autopilot. As commercial boards do not allow the modification of control laws already implemented, a custom-made autopilot has been designed and produced (see Fig. 2). PID control method was initially considered for its simplicity and ease of tuning, its first application concerned the control of a quadrotor UAV [16]. Main characteristics comprehend an open architecture, the possibility to be reprogrammed in flight and real time telemetry. Sensors include GPS, barometric sensor, differential pressure sensor and three-axis gyros and accelerometers. The CPU is the AtMega 1280 model with 128Kb flash memory and 8Kb of RAM.

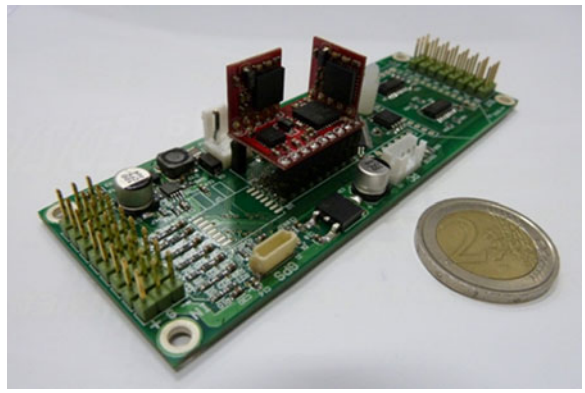

Fig. 2 The autopilot board

3 L1 Adaptive Controller

The choice of the $\mathcal{L}_1$ adaptive controller for the aircraft control is motivated by the high level of uncertainty which generally characterizes UAVs. The $\mathcal{L}_1$ adaptive controller here applied, extensively described in [13], takes into account unmatched uncertainties which include unmodeled dynamics and state- and time-dependent nonlinearities. The adaptive law is a piecewise constant law, as explained in [17, 18], that guarantees fast estimation, the adaptation rate can be associated with the sampling rate of the autopilot board CPU. Moreover, this adaptive algorithm guarantees bounded inputs and outputs, uniform transient response and steady-state tracking. This extension of the $\mathcal{L}_1$ controller was applied to NASA's AirSTAR [19] and to the Boeing X-48B [20]. A key feature of this controller, as explained in the previous works, is that the hardware interface is executed at a lower rate (about 10–100 Hz) than the control algorithm (about 100–1000 Hz), therefore demanding insignificant CPU power. Thus, the computational power can be used for fast adaptation.

The above described controller is designed to control the general linear system of Eq. 4 which, considering uncertainties, can be rewritten as

$$\begin{aligned}
\dot{x}(t) &= A_m x(t) + B_m \omega u(t) + f(x(t), z(t), t), \\
&\quad x(0) = x_0, \\
z(t) &= g_o(x_z(t), t), \;\; \dot{x}_z(t) = g(x_z(t), x(t), t), \\
&\quad x_z(0) = x_{z0}, \\
y(t) &= Cx(t). \qquad (1)
\end{aligned}$$

The matrix $A_m \in R^{n\times n}$ is Hurwitz and specifies the desired dynamics of the closed-loop system, $B_m \in R^{n\times m}$ and $C \in R^{m\times n}$ are known constant matrices. Compared to system (4), system (1) includes $\omega \in R^{m\times m}$ the unknown frequency gain matrix, $z(t)$ and $x_z(t)$ respectively the output and state vector of internal unmodeled dynamics and the unknown nonlinear functions $f(\cdot)$, $g(\cdot)$ and $g_0(\cdot)$.

Another form for the first line of system (1) is

$$\begin{aligned}
\dot{x}(t) &= A_m x(t) + B_m(\omega u(t) + f_1(x(t), z(t), t)) \\
&\quad + B_{um} f_2(x(t), z(t), t), \;\; x(0) = x_0, \qquad (2)
\end{aligned}$$

with $B_{um} \in R^{n\times(n-m)}$ is constant matrix such that $B_m^T B_{um} = 0$ and the rank of $B = [B_m \; B_{um}]$ is n. The unknown nonlinear functions $f_1(\cdot)$ and $f_2(\cdot)$ satisfy the condition

$$\begin{bmatrix} f_1(x(t), z(t), t) \\ f_2(x(t), z(t), t) \end{bmatrix} = B^{-1} f(x(t), z(t), t).$$

The state predictor is defined as

$$\begin{aligned}
\dot{\hat{x}}(t) &= A_m \hat{x}(t) + B_m(\omega_0 u(t) + \hat{\sigma}_1(t)) + B_{um}\hat{\sigma}_2(t), \\
&\quad \hat{x}(0) = x_0
\end{aligned}$$

where $\hat{\sigma}_1(t) \in R^m$ and $\hat{\sigma}_2(t) \in R^{n-m}$, with ω_0 a suitable value for ω. The adaptation laws are

$$\begin{bmatrix} \hat{\sigma}_1(t) \\ \hat{\sigma}_2(t) \end{bmatrix} = -\begin{bmatrix} \mathbb{I}_m & 0 \\ 0 & \mathbb{I}_{n-m} \end{bmatrix} B^{-1}\Phi^{-1}(T_s)\mu(iT_s), \qquad (3)$$

for $i = 0, 1, 2, \ldots,$ and $t \in [iT_s, (i+1)T_s]$, where $T_s > 0$ is the adaptation sampling time associated with the sampling rate of the CPU installed on the autopilot board. In Eq. 3 also appear

$$\begin{aligned}
\Phi(T_s) &= A_m^{-1}\left(e^{A_m T_s} - \mathbb{I}_n\right), \in R^{n\times n} \\
\mu(iT_s) &= e^{A_m T_s}\tilde{x}(iT_s),
\end{aligned}$$

where $\tilde{x}(t) = \hat{x}(t) - x(t)$ is the error between the system state and the predicted state.

Finally, the last element of the controller is the control law defined as

$$u(t) = -K\chi(t).$$

Calling s the complex argument resulting from the Laplace transform of the corresponding time domain signal, it is possible to define

$$\begin{aligned}
\chi(s) &= D(s)\hat{\eta}(s), \\
\hat{\eta}(t) &= \omega_0 u(t) + \hat{\eta}_1(t) + \hat{\eta}_{2m}(t) - r_g(t), \\
\hat{\eta}_1(t) &= \hat{\sigma}_1(t), \\
\hat{\eta}_{2m}(s) &= H_m^{-1}(s)H_{um}(s)\hat{\sigma}_2(s), \\
r_g(s) &= K_g(s)r(s).
\end{aligned}$$

$D(s)$ is a proper stable transfer matrix of dimension $m \times m$, $r(t)$ is the reference signal. The

transfer functions H_m and H_{um} are calculated starting from the matrices of systems (1) and (2)

$$H_m(s) = C(s\mathbb{I}_n - A_m)^{-1}B_m$$

$$H_{um}(s) = C(s\mathbb{I}_n - A_m)^{-1}B_{um}$$

while the prefilter $Kg(s)$ is chosen as the constant matrix $K_g = -(CA_m^{-1}B_m)^{-1}$ to achieve decoupling among the signals.

4 Implementation and Simulation Results

The $\mathcal{L}_1$ adaptive controller is designed on the linear model of the aircraft which separates the longitudinal and latero-directional planes. Final tests are carried out on the nonlinear model which better represents the behavior of the real aircraft.

The $\mathcal{L}_1$ controller is chosen for the control of the inner navigation loops that need a faster response and are more prone to be affected by unmodeled uncertainties. The controlled variables include the pitch angle θ, the longitudinal component of the airspeed u and the roll angle ϕ. Altitude h and heading ψ outer navigation loops are instead controlled by simple PIDs. Figure 3 represents the global control scheme and highlights the control actions and the controlled variables. In the scheme $\overline{y}$ represents all the longitudinal and latero-directional states as they will be defined in Eqs. 5 and 6.

4.1 Linear Case

The $\mathcal{L}_1$ adaptive controller parameters are designed on the linear decoupled model of the aircraft. Reference flight conditions for the model building are speed $V_0 = 13.5$ m/s, altitude $h_0 = 100$ m, angle of attack $\alpha_0 = 5.18$ deg and $\theta_0 = 5.18$ deg. The equations of motion linearization

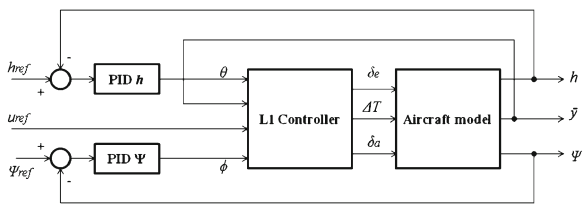

Fig. 3 The control scheme

procedure results in the decoupling of the longitudinal and latero-directional planes. Each of them is modeled with standard continuous time-invariant state space representation

$$\dot{x}(t) = Ax(t) + Bu(t),$$
$$y(t) = Cx(t), \tag{4}$$

where $x(t)$ is the state vector, $u(t)$ the control signal, $y(t)$ the controlled output, A the state matrix, B the input matrix and C the output matrix. Matrices A, B and C are built according to [21], the aerodynamic derivatives in the matrices are obtained by a validated software based on the extended lifting-line theory.

The state variables in the longitudinal plane are the longitudinal component of the total airspeed u, the angle of attack α, the pitch angle θ and the pitch rate q; the controls are the throttle ΔT acting on u and the elevator deflection δ_e acting on θ. The resulting state space elements are

$$x_{\text{lon}}(t) = \left[u,\ \alpha,\ \theta,\ q\right]^T \in R^{n_{\text{lon}}},$$
$$u_{\text{lon}}(t) = [\delta T, \delta_e]^T \in R^{m_{\text{lon}}},$$
$$A_{\text{lon}} \in R^{n_{\text{lon}} \times n_{\text{lon}}},$$
$$B_{\text{lon}} \in R^{n_{\text{lon}} \times m_{\text{lon}}},$$
$$C_{\text{lon}} \in R^{m_{\text{lon}} \times n_{\text{lon}}} \tag{5}$$

with $n_{\text{lon}} = 4$ and $m_{\text{lon}} = 2$. The state matrix A_{lon} is Hurwitz. The short period mode has natural frequency $\omega_{\text{SP}} = 16.6$ rad/s and damping $\zeta_{\text{SP}} = 0.49$, while phugoid mode has natural frequency $\omega_{\text{PH}} = 0.91$ rad/s and damping $\zeta_{\text{PH}} = 0.045$.

The latero-directional states are the lateral component of the total airspeed v, the roll rate p, the yaw rate r and the roll angle ϕ; the only control is the aileron deflection δ_a acting on ϕ. The latero-directional state space elements are

$$x_{\text{lat}}(t) = \left[v,\ p,\ r,\ \phi\right]^T \in R^{n_{\text{lat}}},$$
$$u_{\text{lat}}(t) = \left[\delta_a\right] \in R^{m_{\text{lat}}},$$
$$A_{\text{lat}} \in R^{n_{\text{lat}} \times n_{\text{lat}}},$$
$$B_{\text{lat}} \in R^{n_{\text{lat}} \times m_{\text{lat}}},$$
$$C_{\text{lat}} \in R^{m_{\text{lat}} \times n_{\text{lat}}} \tag{6}$$

with $n_{\text{lat}} = 4$ and $m_{\text{lat}} = 1$. The state matrix A_{lat} has one real and negative eigenvalue corresponding

to a stable roll mode, one real and positive eigenvalue showing a slightly unstable spiral mode, and a couple of complex conjugate eigenvalues for the Dutch Roll characterized natural frequency $\omega_{DR} = 5.9$ rad/s and damping $\zeta_{DR} = 0.12$.

The desired dynamics are chosen to optimize the closed-loop response in terms of rise time, settling time and overshoot. On the longitudinal plane two oscillating modes are defined, one with high natural frequency and damping ($\omega_1 = 8$ rad/s and $\zeta_1 = 0.9$) representing the short period, another representing the phugoid with lower natural frequency and damping ($\omega_2 = 3$ rad/s and $\zeta_2 = 0.8$). On the latero-directional plane two real negative eigenvalues are chosen ($\lambda_1 = -6$ and $\lambda_2 = -10$), the desired oscillating mode representing the dutch roll is defined by $\omega_3 = 5$ rad/s and $\zeta_3 = 0.5$. Note that all filters applied in the controller are represented by first order transfer functions. All simulations are performed using MathWorks Simulink software tool.

The results for the linear model are initially validated considering an autopilot configuration based on PID controllers for both the inner and outer loops. A multi-loop PID commercial autopilot was integrated on the MH850 UAV with the goal of satisfying nominal stability, nominal performance, robust stability and robust performance requirements (details of the project can be found in [22]. Similarly to the present case, in the longitudinal plane the airspeed u is controlled by the throttle ΔT, while the altitude is controlled by the elevator δ_e. Note that in paper [22] the airspeed u was controlled by the elevator δ_e and the altitude was controlled by the throttle ΔT. Three PID controllers are set, two feedbacks on the speed loop (pitch angle θ and airspeed u) and one on the altitude loop (altitude h). In the latero-directional plane ailerons δ_a control the heading ψ through two feedbacks on the roll ϕ and heading angle ψ. This PID control scheme is applied to the same linear model here described, confrontation with the $\mathcal{L}_1$ responses is presented.

Results of the inner loop control are depicted in Fig. 4. Reference signals comprehend a step input for the speed and a doublet input for the pitch and for the roll angle, all starting at different times. The $\mathcal{L}_1$ controlled outputs show an excellent tracking of the reference signals, a mild coupling effect is visible on the pitch response when longitudinal airspeed is increased. PID controlled variables show better tracking performance only for the pitch angle θ, while for u and ϕ the $\mathcal{L}_1$ controller is preferable.

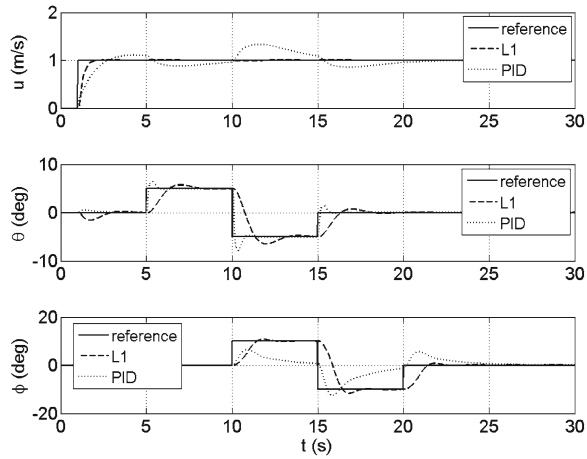

Fig. 4 Linear model inner variables, $\mathcal{L}_1$ and PID confrontation

The complete control scheme includes two PID controllers dedicated to altitude and heading angle control. Their tuning is carried out through an hybrid approach based on root locus plot and H_∞ loop shaping method, the purpose is to obtain good transient responses and satisfying robust properties. Step inputs with typical values for the aircraft considered are given as reference signals, results are shown in Fig. 5. For $\mathcal{L}_1$ slower but

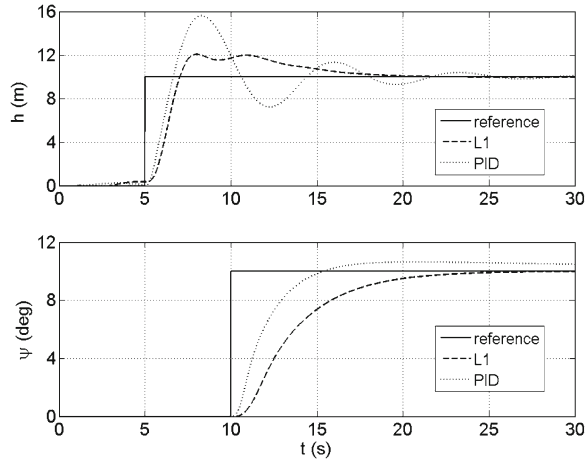

Fig. 5 Linear model outer variables, $\mathcal{L}_1$ and PID confrontation

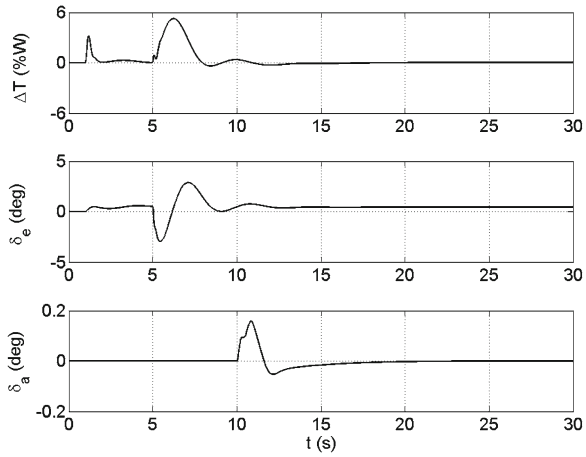

Fig. 6 Linear model $\mathcal{L}_1$ control input

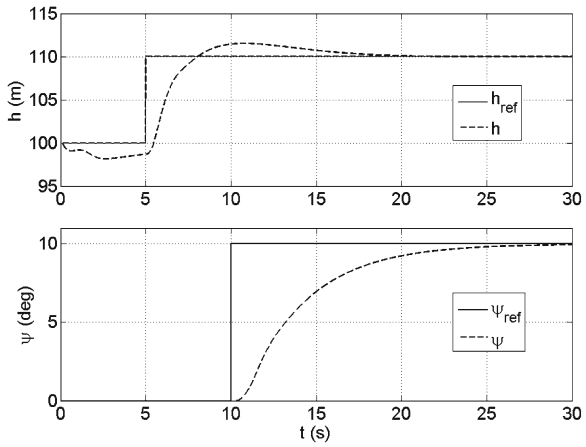

Fig. 8 Nonlinear model outer loop $\mathcal{L}_1$ time responses

still satisfying responses are obtained for the outer loop controlled variables h and ψ, some mild coupling effects appear on the speed u. PID control scheme shows lower performances in terms of overshoot, damping and steady state error.

The corresponding $\mathcal{L}_1$ control inputs appear in Fig. 6. The throttle is expressed as percentage of the aircraft weight W, elevator command δ_e and aileron command δ_a remain under the imposed command saturation limit of 25 degrees.

4.2 Nonlinear Case

The controller parameters, tuned for the decoupled linear model, are validated considering a complete nonlinear model obtained from the aircraft equations of motion as defined in [23]. These are a set of 12 equations describing the forces, moments, angles and angular speeds which characterize the flight condition of the aircraft. Trim conditions coincide with the equilibrium values used for the linear model (Section 4.1).

The same reference perturbations of the linear case are applied starting from the following equilibrium conditions: $V_0 = 13.5$ m/s, $\theta_0 = 5.18$ deg, $h_0 = 100$ m, $\phi_0 = 0$ deg and $\psi_0 = 0$ deg. Results appear in Fig. 7. Tracking capabilities are maintained despite some initial oscillations in the longitudinal variables which damp after few seconds. No coupling between longitudinal and latero-directional planes is observable despite the nonlinear model does not separate them.

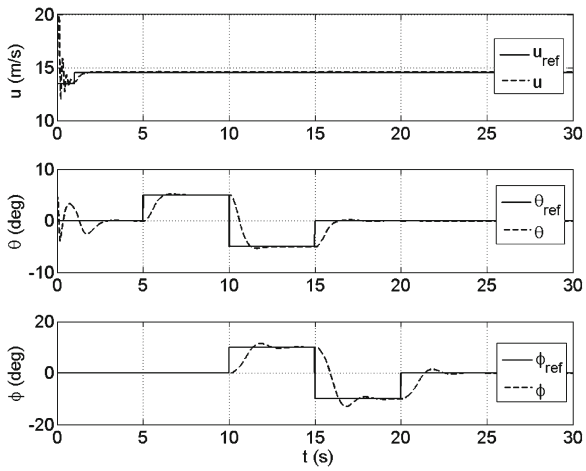

Fig. 7 Nonlinear model inner loop $\mathcal{L}_1$ time responses

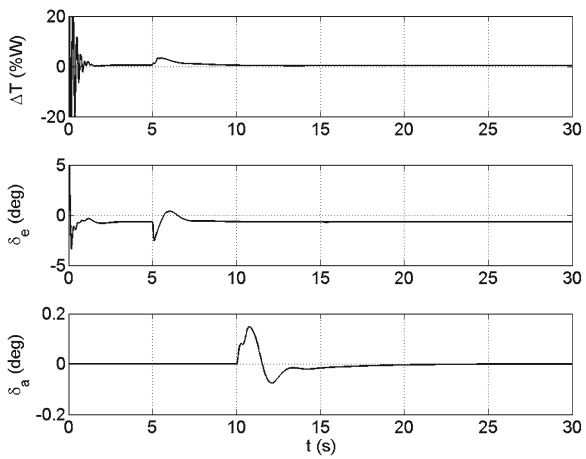

Fig. 9 Nonlinear model control input

Table 1 Aircraft parameters variation

Parameter	Nominal value	Range of variation
m	900 g	720–1080 g
V	13.5 m/s	10.8–16.2 m/s
J_x	0.011 kg·mm^2	0.0088–0.0132 kg·mm^2
J_y	0.012 kg·mm^2	0.0096–0.0144 kg·mm^2
J_z	0.022 kg·mm^2	0.0176–0.0264 kg·mm^2
J_{xz}	$4.6 \cdot 10^{-5}$ kg·mm^2	3.68–5.52·10^{-5} kg·mm^2

Finally results for the complete controller are represented in Fig. 8. Satisfying responses are obtained, in line with the results of the linear case. The corresponding control actions are plotted in Fig. 9. Comparing with the linear case, the aileron action remains unchanged. On the longitudinal plane, during the initial seconds oscillations appear, in particular for the throttle. The remaining of the simulation shows a control action similar in trend but characterized by a lower magnitude. Note that no parameters of both $\mathcal{L}_1$ and PID controllers were changed passing from the linear to the nonlinear case.

4.3 Validation

Variations on total airspeed V_0 and aircraft mass m_0 to take into account wind and changes in payload mass are considered. Uncertainties of inertial data J_x, J_y, J_z, J_{xz} model manufacturing inaccuracies. A combined variation of ±20 % of these variables is considered to validate the adaptive $\mathcal{L}_1$ controller in the complete control scheme case. The same input signals previously analyzed are considered. In addition to the variables already plotted in Figs. 4, 5, 6, 7, and 8, here the angle of attack α, the lateral speed v, the angular pitch, roll and yaw rates p, q, r are also analyzed (Table 1).

Figures 10, 11, and 12 represent the effects on the linear model. No significant alterations are observable, the controller proves to be able to deal with these substantial variations without problems. A different total speed V will result in a different steady state angle of attack α to adapt to the new equilibrium condition. For all the other variables nominal and perturbed values converge to the same steady state value. Among the three

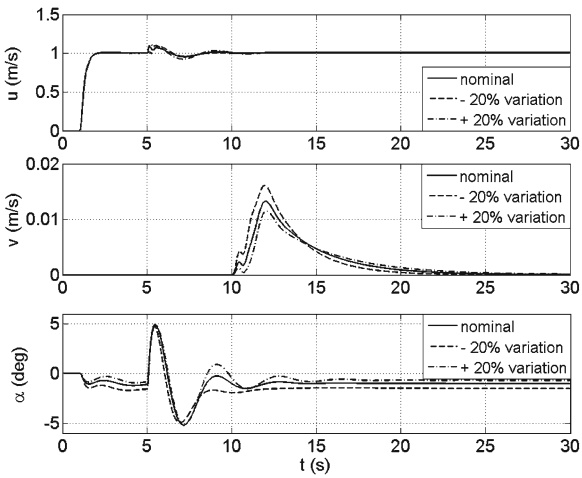

Fig. 10 Linear model u, v and α $\mathcal{L}_1$ time responses

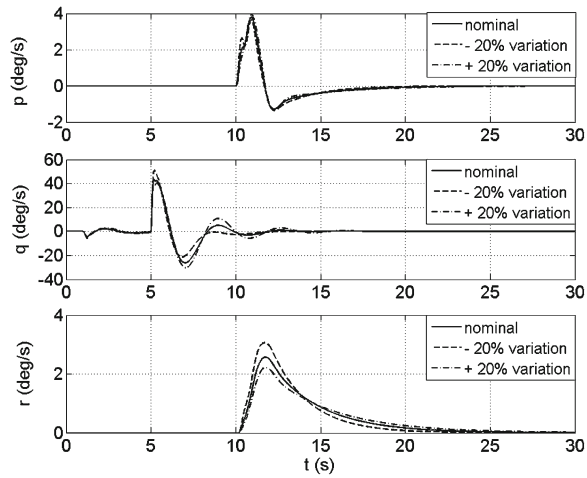

Fig. 11 Linear model p, q and r $\mathcal{L}_1$ time responses

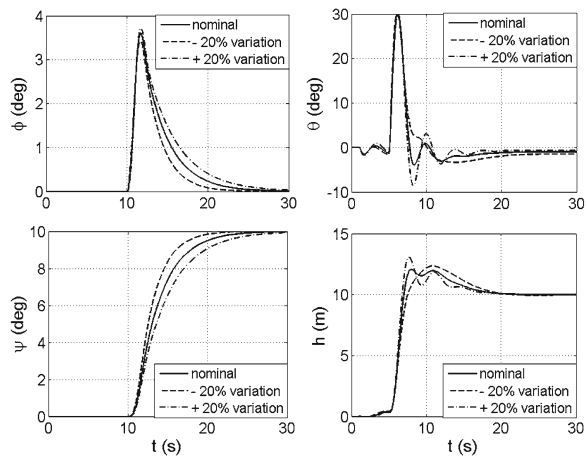

Fig. 12 Linear model ϕ, θ, ψ and h $\mathcal{L}_1$ time responses

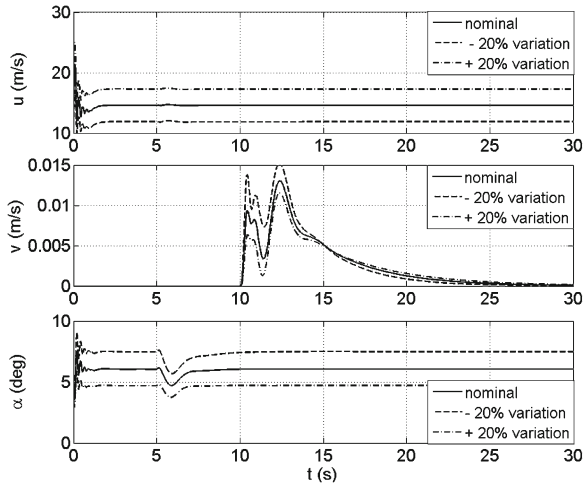

Fig. 13 Nonlinear model u, v and α $\mathcal{L}_1$ time responses

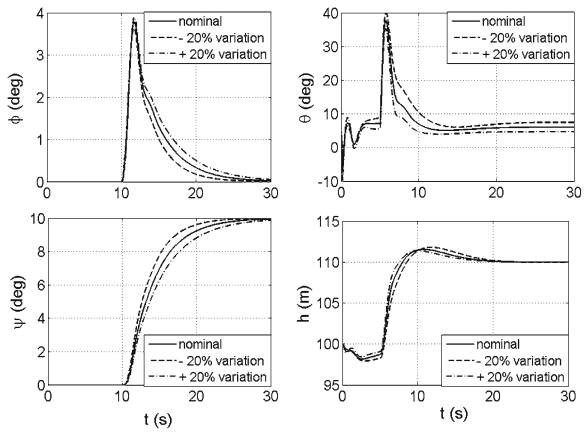

Fig. 15 Nonlinear model ϕ, θ, ψ and h $\mathcal{L}_1$ time responses

controlled variables the altitude h is the one more affected by the parameters variation as oscillations appear.

The nonlinear case appears in Figs. 13, 14, and 15. Initial oscillations aside, the nonlinear model does not seem to be more concerned by the perturbations. Differently from the linear model, the u plot is different as three steady state values are observable. The reason of this result is found in the different approach which characterizes linear and nonlinear simulation. In the linear case the reference signal is a perturbation of the equilibrium condition at which state space matrices are calculated. In the nonlinear case the reference signal indicates the value that the controlled variable has to follow. Thus in the linear case the 1 m/s step input indicates just the increase in longitudinal speed starting from three different values of V, $V_0 = 13.5$ m/s and $V_0 = 13.5 \pm 20$ % m/s. In the nonlinear case, instead, the values of the three speeds are drawed.

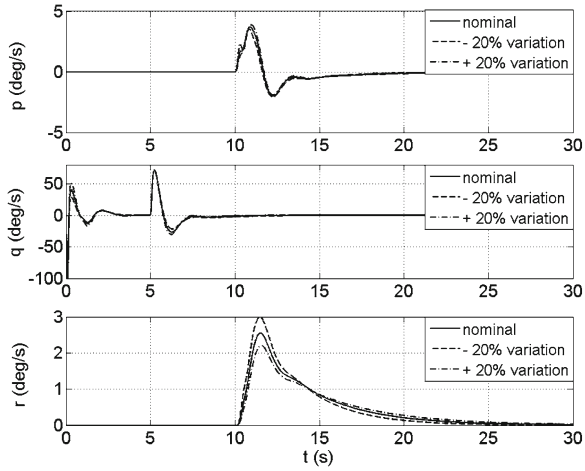

Fig. 14 Nonlinear model p, q and r $\mathcal{L}_1$ time responses

5 Conclusions

In this paper an $\mathcal{L}_1$ adaptive algorithm used as autopilot inner loop controller is analyzed. Two models are considered, a state space linear model defined for specific flight conditions and a nonlinear model based on the equations of motion. PID control laws are applied in both models for altitude and heading outer loop tracking. The global controller parameters are tuned on the linear decoupled model and validated for the nonlinear model. The paper demonstrates that, if an $\mathcal{L}_1$ algorithm is considered for the inner loop, no retuning or gain scheduling is required, even if a nonlinear complete system is considered. Moreover, the same PID gains can be used both for the low fidelity and high fidelity models. Finally, the employed controller is especially designed for the implementation on autopilot boards. Its adaptation rate is compatible with standard CPU clock time and it requires low computational effort.

Future developments will include the implementation of the adaptive controller on a customized

autopilot board to experimentally verify the obtained results. A refinement of the engine and propeller models are also envisaged to cope with the complexity of these important components of the aircraft which can substantially affect the aircraft dynamics.

Acknowledgements The authors thank the Prof. Naira Hovakimyan and her group at the University of Urbana—Champaign (Illinois, USA) for sharing experience and knowledge on the $\mathcal{L}_1$ controller theory and implementation.

References

1. Chao, H.Y., Cao, Y.C., Chen, Y.Q.: Autopilots for small unmanned aerial vehicles: a survey. Int. J. Control. Autom. Syst. **8**(1), 36–44 (2010)
2. Åström, K.J., Hägglund, T.: PID Controllers: Theory, Design, and Tuning. Instrument Society of America, Triangle (1995)
3. Cominos, P., Munro, N.: PID controllers: recent tuning methods and design specification. IEE Proc. Control Theory Appl. **149**(1), 46–53 (2002)
4. Ho, M.T.: Synthesis of $H_0\infty$ PID controllers: a parametric approach. Automatica **39**(1), 1069–1075 (2003)
5. Ntogramatzidis, L., Ferrante, A.: Exact tuning of PID controllers in control feedback design. IET Control Theory Appl. **5**(4), 565–578 (2011)
6. Schumacher, C., Kumar, R.: Adaptive control of UAVs in close-coupled formation flight. Proc. Am. Control Conf. **2**, 849–853 (2000)
7. Moon, J., Sattigeri, R., Prasad, J.V.R., Calise, A.J.: Adaptive guidance and control for autonomous formation flight. In: American Helicopter Society 63rd Annual Forum (2007)
8. Shin, D.H., Kim, Y.: Reconfigurable flight control system design using adaptive neural networks. IEEE Trans. Control Syst. Technol. **12**(1), 87–100 (2004)
9. Farrell, J., Polycarpou, M., Sharma, M.: Adaptive backstepping with magnitude, rate, and bandwidth constraints: Aircraft longitude control. Proc. Am. Control Conf. **5**, 3898–3904 (2003)
10. Matthews, J.S., Knoebel, N.B., Osborne, S.R., Beard, R.W., Eldredge, A.: Adaptive backstepping control for miniature air vehicles. In: Proceedings of the 2006 American Control Conference, Minneapolis, 14–16 June (2006)
11. Beard, R.W., Knoebel, N.B., Cao, C., Hovakimyan, N., Matthews, J.S.: An $\mathcal{L}_1$ adaptive pitch controller for miniature air vehicles. In: AIAA Guidance, Navigation, and Control Conference and Exhibit, Keystone, 21–24 August (2006)
12. Cao, C., Hovakimyan, N.: Design and analysis of a novel $\mathcal{L}_1$ adaptive control architecture with guaranteed transient performance. IEEE Trans. Automat. Contr. **53**(2), 586–591 (2008)
13. Hovakimyan, N., Cao, C.: $\mathcal{L}_1$ Adaptive Control Theory. Society for Industrial and Applied Mathematics, Philadelphia (2010)
14. Marguerettaz, P., Sartori, D., Guglieri, G., Quagliotti, F.: Design and development of a man-portable unmanned aerial system for alpine surveillance missions. Presented at UAS International 2010, Paris, France (2010)
15. Capello, E., Guglieri, G., Marguerettaz, P., Quagliotti, F.: Preliminary assessment of flying and handling qualities for mini-UAVs. J. Intell. Robot. Syst. **65**, 43–61 (2012)
16. Capello, E., Scola, A., Guglieri, G., Quagliotti, F.: A mini quadrotor UAV: design and experiment. J. Aerosp. Eng. ASCE (2012). doi:10.1061/(ASCE)AS.1943-5525.0000171
17. Cao, C., Hovakimyan, N.: $\mathcal{L}_1$ adaptive output-feedback controller for non-strictly-positive-real reference systems: missile longitudinal autopilot design. AIAA J. Guid. Control Dyn. **32**, 717–726 (2009)
18. Xargay, E., Hovakimyan, N., Cao, C.: $\mathcal{L}_1$ adaptive controller for multi-input multi-output systems in the presence of nonlinear unmatched uncertainties. In: Proceedings of American Control Conference, pp. 875–879 (2010)
19. Gregory, I.M., Xargay, E., Cao, C., Hovakimyan, N.: Flight test of $\mathcal{L}_1$ adaptive control on the NASA AirSTAR flight test vehicle. In: AIAA Guidance, Navigation and Control Conference, Toronto (2010)
20. Leman, T., Xargay, E., Dullerud, G., Hovakimyan, N.: $\mathcal{L}_1$ adaptive control augmentation system for the X-48B aircraft. In: AIAA Guidance, Navigation and Control Conference, Chicago (2009)
21. Stevens, B.L., Lewis, F.L.: Aircraft Control and Simulation, 2nd edn. Wiley, New York (2003)
22. Capello, E., Sartori, D., Guglieri, G., Quagliotti, F.B.: Robust assessment for the design of multi-loop PID autopilot. Accepted for Pubblication on IET Control Theory and Applications (2012)
23. Etkin, B., Reid, L.: Dynamics of Flight: Stability and Control, 3rd edn. Wiley, New York (1996)